OVERVIEW

Molecular modeling and dynamics studies with explicit inclusion of electronic polarizability: theory and applications

**Pedro E. M. Lopes · Benoit Roux ·
Alexander D. MacKerell Jr**

Abstract A current emphasis in empirical force fields is on the development of potential functions that explicitly treat electronic polarizability. In the present article, the commonly used methodologies for modeling electronic polarization are presented along with an overview of selected application studies. Models presented include induced point-dipoles, classical Drude oscillators, and fluctuating charge methods. The theoretical background of each method is followed by an introduction to extended Lagrangian integrators required for computationally tractable molecular dynamics simulations using polarizable force fields. The remainder of the review focuses on application studies using these methods. Emphasis is placed on water models, for which numerous examples exist, with a more thorough discussion presented on the recently published models associated with the Drude-based CHARMM and the AMOEBA force fields. The utility of polarizable models for the study of ion solvation is then presented followed by an overview of studies of small molecules (e.g., CCl_4, alkanes, etc.) and macromolecule (proteins, nucleic acids and lipid bilayers) application studies. The review is written with the goal of providing a general overview of the current status of the field and to facilitate future application and developments.

P. E. M. Lopes · A. D. MacKerell Jr (✉)
Department of Pharmaceutical Sciences, School of Pharmacy,
University of Maryland, 20 Penn Street,
Baltimore, MD 21230, USA
e-mail: alex@outerbanks.umaryland.edu

B. Roux
Institute of Molecular Pediatric Sciences,
Gordon Center for Integrative Science, University of Chicago,
929 E. 57th St., Chicago, IL 60637, USA

1 The need for polarizable force fields

Molecular mechanical (MM) or empirical force fields are widely used in molecular modeling and dynamics studies of biological and materials systems that contain 100,000 or more atoms. This capability is based on the utilization of simplified potential energy functions for determination of the energies and forces acting on large heterogeneous systems. However, such simplified forms of the energy function are also a weakness of MM methods as they limit their inherent accuracy. One of the major limitations with respect to the accuracy of the majority of current MM force fields is the way in which the charge distribution of the molecules is treated. Typically, effective partial fixed charges are assigned to the atoms independent of the environment, which are adjusted to account for the influence of induced polarization in an average way. The functional form of the Coulomb interaction potentials thus created is not capable of adapting the charge distributions to changes of polarity in the environment. Such force fields, which are commonly termed "additive", are currently used for most biomolecular simulations [1–5]. These force fields all share the same functional form to determine the potential energy as a function of the geometry, $U(\mathbf{r})$:

$$U(\mathbf{r}) = U_{\text{bond}}(\mathbf{r}) + U_{\text{vdW}}(\mathbf{r}) + U_{\text{elect}}(\mathbf{r}) \qquad (1a)$$

$$U_{\text{elect}}(\mathbf{r}) = \sum_{i=1}^{N} \sum_{j \neq i} \frac{q_i q_j}{r_{ij}} \qquad (1b)$$

In Eqs. 1a and 1b, $U_{\text{bond}}(\mathbf{r})$ represents the bonded terms (bonds, valence angles, dihedral or torsion angles, etc.),

U_{vdW} (**r**) represents the van der Waals (vdW) contribution, typically being a Lennard–Jones (LJ) 6–12 term, and U_{elect} (**r**) is the electrostatic interaction term of the Coulomb form (Eq. 1b), where q_i and q_j are the partial atomic charges of atoms i and j separated by a distance, r_{ij}. While the functional form in Eqs. 1a and 1b has been widely used (e.g., the CHARMM [3], AMBER [2] and OPLS [6] force field papers in combination have been cited over 8,500 times) the inability of the charge distribution to vary and adapt as a function of the local electric field is considered a major limitation of current models, significantly diminishing their ability to accurately treat intermolecular interactions in a variety of environments [7–10]. Accordingly, it has become clear that the inclusion of electronic polarization will play a central role in the next generation of force fields for molecular dynamics (MD) and Monte Carlo (MC) simulations [11, 12].

In simple terms it is known that the molecular dipole moment of individual molecules change significantly when they are transferred from the gas to liquid phase. A prime example of the importance of electronic polarization to reproduce these phenomena is the dipole moment of water in different environments. In the gas phase, an isolated water molecule has a dipole moment of 1.85 D [13], but the average molecular dipole is 2.1 D in the water dimer and increases in larger water clusters [14]. In the condensed phase it reaches, a value between 2.4 and 2.6 D, as suggested from classical MD simulations of the dielectric properties [15–17], and 2.95 D, a value obtained from ab initio MD simulations [18–20] and from analysis of experimental data [21, 22]. This bulk value is close to the maximum dipole any charged or polar molecule can induce in a water molecule. For example, the presence of a sodium ion or a dimethyl phosphate anion in bulk water does not significantly add to the induction effect that occurs in pure water [23].

By explicitly including polarization, a force field may be parameterized to reproduce accurate gas-phase quantum mechanical (QM) or experimental data and also perform well in condensed phases, due to the fact that it is able to respond to environmental effects. According to Rayleigh–Schrödinger QM perturbation theory, a dipole linearly proportional to the local electric field from the environment is induced in the molecule. Thus, if the electric field is not too large, such that hyperpolarization effects are absent, the induced dipole $\boldsymbol{\mu}$ on an atom is the product of the total electric field **E** and the atomic polarizability $\boldsymbol{\alpha}$.

$$\boldsymbol{\mu} = \boldsymbol{\alpha} \cdot E \tag{2}$$

The total electric field, **E**, is composed of the external electric field, $\mathbf{E}^0$, from the permanent atomic charges and the contribution from other induced dipoles. This is the basis of most polarizable force fields currently being developed for biomolecular simulations. Methods for this treatment of polarizability will be discussed in more detail in the following section.

It should be noted that the present review is biased towards the polarizable force fields implemented in the program CHARMM and towards applications to systems of biological interest. To all groups active in developing polarizable force fields and not referenced in this work, the authors wish to express their apologies. Much of the work not covered in the present review has been described in the special issue of the *Journal of Chemical Theory and Computation* dedicated to polarization [24].

2 Methodologies commonly used for polarizable biomolecular simulations

2.1 Induced dipole model

One method for treating polarizability consists of including both partial atomic charges and inducible dipoles on the atoms comprising the molecular system. In the most common variation currently in use [25–29], point inducible dipoles are added to some or all atomic sites while in the methodology proposed by Allinger and co-workers bond dipoles, in combination with atomic charges, are considered [30]. In the induced dipole approach the dipole moment, $\boldsymbol{\mu}$, induced on a site i is proportional to the electric field at that site, $\mathbf{E}_i$. The proportionality constant is the polarizability tensor, $\boldsymbol{\alpha}$. The dipole feels an electric field both from the permanent charges of the system and from the other induced dipoles. The expression for $\boldsymbol{\mu}$ is

$$\boldsymbol{\mu}_i = \boldsymbol{\alpha}_i \cdot E_i = \boldsymbol{\alpha}_i \cdot \left[E_i^0 - \sum_{j \neq i} T_{ij} \boldsymbol{\mu}_j \right] \tag{3}$$

where $\mathbf{E}^0$ is the field from the permanent charges and $\mathbf{T}_{ij}$ is the dipole field tensor.

A feature of the induced dipole polarizable model, as well as all polarizable models, is that the assignment of the electrostatic parameters is in principle easier than for additive models. Charges can be assigned based on experimental gas phase dipole moments or can be determined using QM ab initio methods and the polarizabilities can be obtained from the literature or QM calculations. For example, seminal work by Thole [31] and Applequist [32] showed how a set of simple polarizabilities based on atom type could reproduce the dipole moments and polarizabilities of a range of molecules. This is in contrast to nonpolarizable models, in which charges are systematically overestimated to have some enhanced permanent dipole moment to reflect the enhanced polarization required to accurately treat condensed phases [2, 33, 34]. Indeed,

determining the degree of charge enhancement is part of the art of constructing additive potentials and constrains the utility of these potentials to a limited range of environments [12, 35].

An implementation of the induced dipole method in CHARMM has been reported [36], based on the polarizable intermolecular potential functions (PIPF) model of Gao and co-workers [37, 38]. The PIPF potential combined with the CHARMM22 force field has been designated PIPF-CHARMM, although the model has not yet been extended to cover all the amino acids. In this model, infinite polarization is avoided by using Thole's electrostatic damping scheme [31, 39]. A method to accelerate the convergence of the induced dipoles for systems employing the PIFF potential functions has been described [40].

An approximation to the induced dipole model was proposed by Ferenczy and Reynolds [41]. This induced charge method involves point charges only, and those depend on the environment. It is based on the idea of representing atomic point dipoles by point charges on neighboring atoms. The method was extended so that both the polarization energy and its derivatives can be determined.

More recently, Ponder and co-workers [42–49] developed the AMOEBA force field based on a modification of the formulation of Applequist and Thole. It uses a modification of Eq. 3 with the static electric field typically treated with permanent atomic charges replaced by permanent multipoles:

$$\boldsymbol{\mu}_i = \boldsymbol{\alpha}_i \cdot E_i = \boldsymbol{\alpha}_i \cdot \left[\sum_{j \neq i} T_{ij}^{\alpha} \mathbf{M}_j + \sum_{k \neq i} T_{ik}^{\alpha\beta} \boldsymbol{\mu}_k \right] \qquad (4)$$

where $\mathbf{M}$ ($M_i = (q_i, \mu_{i,x}, \mu_{i,y}, \mu_{i,z}, Q_{i,xx}, Q_{i,xy}, Q_{,xz}, \ldots, Q_{i,zz})^{\mathrm{T}}$) is the vector of permanent atomic multipole components, up to quadrupole, and $\mathbf{T}$ is the interaction matrix. Accordingly, the induced atomic dipoles must respond to the contribution of the multipoles as well as the contribution of the other induced dipoles to the electric field. While such an extension represents an increased computational demand, the inclusion of atomic multipoles more accurately treats the interactions between molecules as a function of orientation, avoiding the inclusion of particle representative of lone pairs as has been incorporated into the CHARMM Drude force field (see below).

2.2 Classical Drude oscillator model

Another method to include polarization consists in modeling the polarizable atomic centers using dipoles of finite length, represented by a pair of point charges. A variety of different models of polarizability have used this approach, but especially noteworthy is the classical Drude oscillator

models (also known as the "shell" or "charge on spring" model) frequently used in simulations of solid state ionic materials and recently extended to water and organic compounds, including biomolecules. The Drude model can trace its origin to the work of Paul Drude in 1902 and was developed as a simple way to describe the dispersive properties of materials [50]. It represents electronic polarization by introducing a massless charged particle, attached to the atomic center of each polarizable atom by a harmonic spring. The position of these "auxiliary" particles is then adjusted self-consistently to their local energy minima for any given configuration of the atoms in the system, thereby taking into account the permanent electric field due to the fixed charges and the contribution of the induced dipoles to the electric field. A quantum version of the model (including the zero-point vibrations of the oscillator) has been used in early applications to describe the dipole–dipole dispersion interactions [51–55]. A semiclassical version of the model was used more recently to describe molecular interactions [56], and electron binding [57]. The classical version of the model has been quite useful in statistical mechanical studies of condensed systems and in recent decades has seen widespread use in MD or MC simulations. Example applications include ionic crystals [58–63], a range of simple liquids [36, 64–70], liquid water [71–77], and the hydration of small ions [78, 79]. In recent years, the Drude model was extended to interface with QM approaches in QM/MM methods [80]. A particularly attractive aspect of the Drude oscillator model is that it preserves the simple particle–particle Coulomb electrostatic interaction, such that its implementation in standard biomolecular simulation programs may be performed in a relatively straightforward way.

In the Drude oscillator model polarization is determined by a pair of point charges separated by a variable distance d. For a given atom with charge q assigned to the atomic center a mobile Drude particle (or Drude oscillator) carrying a charge q_D is introduced. The charge on the atom is replaced by $q - q_D$ in order to preserve the net charge of the atom–Drude oscillator pair. The Drude particle is harmonically bound to the atomic particle with a force constant k_D. The mathematical formulation of the Drude model is, in fact, an empirical method of representing the dipolar polarization of the atomic center on which it is introduced. A related method to introduce polarization in FF simulations was developed by Sprik and Klein [148, p. 97], where polarization is represented by closely spaced point charges. In their water model, four charges are placed around the oxygen in addition to the three permanent charges on the oxygen and hydrogen atoms. The introduction of many rigid point charges makes this approach computationally more expensive though it may possibly be more stable since there are no moving particles.

In the absence of an electric field during an MD simulation, the Drude particle oscillates around the position of the atom, **r**, and the atom appears on average as a point charge of magnitude q. In the presence of a uniform field **E**, the Drude particle oscillates around a displaced position **r** + **d**. The Drude separation **d** is related to k_D, **E** and q_D:

$$\mathbf{d} = \frac{q_D \mathbf{E}}{k_D} \tag{5}$$

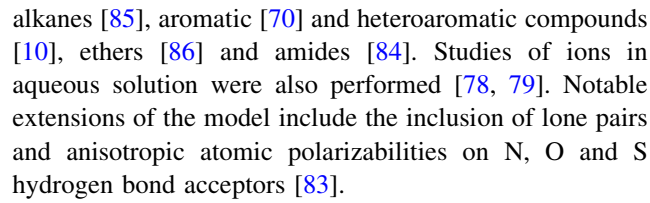and the formula for the induced atomic dipole, **μ**, as a function of **E** is

$$\boldsymbol{\mu} = \frac{q_D^2 \mathbf{E}}{k_D} \tag{6}$$

which results in a simple expression for the isotropic atomic polarizability, α:

$$\alpha = \frac{q_D^2}{k_D} \tag{7}$$

Therefore, in the Drude polarizable model the only relevant parameter is the combination q_D^2/k_D that is responsible for the atomic polarizability. It is of utility to reiterate that the electrostatic interaction in the Drude model is implemented using only the Coulombic term (Eq. 1b) already present in MM simulation codes. No new interaction types, such as the dipole field tensor $\boldsymbol{T}_{ij}$ of Eq. 3 are required. The great practical advantage of not having to compute the dipole–dipole interactions is balanced by the extra charge–charge calculations. However, significant computational savings may be gained in the Drude model by only attaching Drude particles to the non-hydrogen atoms that dominate the molecular polarizability, thereby increasing the total number of interactions pairs by a factor much smaller than 2 [70, 76].

The polarizable Drude model in CHARMM under development in our laboratories is geared towards proteins, lipids, and nucleic acids [68–70, 76–79, 81–84]. Important progress has been made thus far. The algorithm has been generically described in Ref. [81] including the formulation for MD simulations based on an extended Lagrangian as required for computational efficiency. A description of extended Lagrangian integrators for MD simulations is done below. Two water models, that are a generalization of the TIP4P model, have been developed and are referred to as the SWM4-DP (Simple Water Model, four-points with Drude polarizability) [76] and SWM4-NDP (Simple Water Model, four-points with negative Drude polarizability) [77]; the later model will act as the basis of the full biomolecular force field. Protocols to determine the partial charges, atomic polarizabilities [82] and atom-based Thole damping factors [83] have been presented and parametrization of a number model compounds representative of biomolecules have been published, including alcohols [69],

alkanes [85], aromatic [70] and heteroaromatic compounds [10], ethers [86] and amides [84]. Studies of ions in aqueous solution were also performed [78, 79]. Notable extensions of the model include the inclusion of lone pairs and anisotropic atomic polarizabilities on N, O and S hydrogen bond acceptors [83].

The parametrization protocol developed for the polarizable Drude model in CHARMM is well defined. A procedure for determining atomic center and Drude charges [82, 83] and atom-based Thole damping factors [84] has been developed and is analogous to work by Friesner and co-workers [25, 35, 87–89]. A series of maps of the electrostatic potential (ESP) that surrounds the model compound monomer are evaluated using QM density functional theory on a set of specified grid points, differing by the presence and/or location of a perturbing ion in the environment surrounding the molecule. Electrostatic parameters are then fitted to minimize the difference between the QM and Drude ESP maps [82, 83]. Optimization of the components of the parameters not dependent of the Drude oscillator positions, namely the bonding and Lennard–Jones terms, are adjusted as described previously for the additive CHARMM force field [34, 90].

2.3 Fluctuating charges model

Polarizability can also be introduced into standard energy functions (Eqs. 1a and 1b) by allowing the values of the partial charges to respond to the electric field of their environment, thereby altering the molecular polarizability. This may be performed by coupling the charges to their environment using electronegativity equalization (EE) or chemical potential equalization (CPE) schemes. This method for treating polarizability has been called the "fluctuating charge" method [27, 91], the "chemical potential (electronegativity) equalization" method [92–107], or the "charge equilibration" method [108–114] and has been applied to a variety of systems. Examples include application to liquid water [91], vapor–liquid equilibrium [115], studies of ions in aqueous solution [116, 117], studies of peptides [88], aqueous solvation of amides [118] and water and cation–water clusters [119]. A practical advantage of this approach is that it introduces polarizability without introducing new interactions. Compared to the Drude model, this can be done using the same number charge–charge interactions as would be present in a non-polarizable simulation. However, while the fluctuating charge model does not introduce any additional terms or particles as compared to additive force fields it does require a significantly shorter integration time step for stable MD simulations [8], leading to a significant increase in computational costs over additive models.

In the fluctuating charge (FC) method [108], as it is commonly referred to in liquid state and biomolecular force field studies [27, 91], variable discrete charges are located on atomic sites within the molecule. Their value is computed, for a given molecular geometry, by minimization of the electrostatic energy. In a multi-molecular system with N_{molec} molecules and each molecule consisting of N_{atom} atoms and N_{site} charged sites, the electrostatic energy, $U_{elect}(r,q)$ is as follows:

$$U_{elect}(r,q) = \sum_{i=1}^{N_{molec}} \sum_{\alpha=1}^{N_{site}} \left[\chi_{i\alpha}^0 q_{i\alpha} + \frac{1}{2} J_{i\alpha i\alpha}^0 q_{i\alpha}^2 \right]$$
$$+ \sum_{i=1}^{N_{molec}} \sum_{\alpha=1}^{N_{site}} \sum_{\beta > \alpha}^{N_{site}} J_{i\alpha i\beta}(r_{i\alpha i\beta}) q_{i\alpha} q_{i\beta}$$
$$+ \sum_{i=1}^{N_{molec}} \sum_{j>1}^{N_{molec}} \sum_{\alpha=1}^{N_{site}} \sum_{\beta > \alpha}^{N_{site}} J_{i\alpha j\beta}(r_{i\alpha j\beta}) q_{i\alpha} q_{j\beta} \quad (8)$$

The energy given by Eq. 8 replaces the Coulomb energy $q_i q_j / r_{ij}$ in Eqs. 1a and 1b. In Eq. 8 χ_α^0 is the "Mulliken electronegativity" and $J_{\alpha\alpha}^0$ is the "absolute hardness;" [120] these terms represent the electrostatic parameters in the fluctuating charge model and are optimized to reproduce molecular dipoles, interactions with water and the molecular polarization response, typically determined from QM calculations [27]. The charges q_i are thus treated as independent variables, and the polarization response is determined by variations in the charges. These charges depend on the interactions with other molecules as well as other charge sites on the same molecule, and will change for every time step or configuration sampled during a simulation.

In most cases, charge is taken to be conserved for each molecule, so there is no charge transfer between molecules. However, in QM charge transfer is an important part of the interaction energy, so there are reasons to remove this constraint [121–125]. Unfortunately, this procedure often leads to large overestimation of the polarizability as the molecular size increases as charge can now flow along covalent bonds at a small energetic cost. Thus, this method is suitable for small molecules but generally not applicable to macromolecules.

A solution to the over-polarization problem was developed in terms based on the concept of atom–atom charge transfer (AACT) [126]. In this approach, the energy is Taylor expanded in terms of charges transferred between atomic pairs within the molecule, rather than in terms of the atomic charges themselves. Similar in spirit is the bond-charge increment (BCI) model [87, 88], which allows for charge to only flow between two atoms that are directly bonded to each other, the method guarantees that the total charge of each set of bonded atoms is conserved. A related approach is the atom–bond electronegativity equalization method (ABEEM) [127–131] which has been developed based on concepts from density functional theory. In this model, the total electronic energy of a molecule in the ground state is a complex function of different quantities: (1) valence-state chemical potential of atom a, bond $a–b$ and lone-pair electrons, lp, (2) valence-state hardness of atom a, bond $a–b$, and lp, (3) partial charges of atom a, bond $a–b$, and lp, and (4) distances between the different atoms, bonds and lone pairs. ABEEM has been successfully incorporated into the intermolecular electrostatic interaction term in MM models of water [132, 133].

The interpretation of the FC model in the framework of QM theory is well defined. It is possible to derive the FC terms from density functional theory, from which the concept of electronegativity equalization arises naturally [134] or, as developed by Field, in terms of semiempirical MO theory [135]. A major difference between the FC and semiempirical MO methods is the arbitrariness in defining the atomic charges. In the FC model the charge on each atom can take any value with the restriction that the sum of atomic charges equals the total molecular charge. In the semiempirical MO methods the atomic charges are limited by the occupation and form of the orbitals. Despite this difference, the connection of the FC and MO methods can be explored to reduce the arbitrariness in the introduction of polarization inherent to the induced dipole or Drude models.

There are other approaches to include polarization in MD simulations. For example, a pure QM based method, conceptually related to the fluctuating charge model, was developed by Gao [136, 137]. Each molecule is treated with a QM method, for example AM1 was used in Ref. [137], and the remaining molecules are represented by a Hartree product of the individual monomer wavefunctions. In this approximation, exchange interactions are neglected and a LJ term is included to compensate.

2.4 Implementation of extended Lagrangian integrators for MD simulations

An essential feature of MM methods for the treatment of biomolecular systems is their computational efficiency. The inclusion of polarizability increases the computational demand due to the addition of dipoles or additional charges centers and, in the context of MD simulations, the requirement for shorter integration timesteps. In addition, for every energy or force evaluation it is necessary to solve for all the polarizable degrees of freedom in a self-consistent manner. Traditionally, this is performed via a self-consistent field (SCF) calculation in which the induced polarization is solved iteratively until a satisfactory level of convergence is achieved [74, 138, 139]; the SCF equation can also be solved in a single step with matrix inversion

[140–142]. While these methods have been widely used they involve significant computational costs (converging the SCF procedure requires about 15 iterations and the inversion of a large matrix is slow), making their use in MD simulations problematic. To overcome this MD integrators have been developed in which the polarizable degrees of freedom are included as dynamic variables. These approaches, whose origins go back to the Carr-Parrinello approach for QM simulations [143], are referred to an extended Lagrangian methods [144–146]. Such approaches have been developed for the majority of polarization methods discussed above. These include implementations for induced dipoles [147], Drude oscillators [81] and fluctuating charge methods [91, 148]. In the case of the Drude oscillator model, it was explicitly demonstrated that the dynamics of an extended Lagrangian system, in which a small mass is attributed to the auxiliary Drude particles and the amplitude of their oscillations away from the local energy minimum is controlled separately with a low-temperature thermostat, provides a close approximation to the SCF regime [81]. The availability of extended Lagrangian methods are central to the future success of MD simulations that include electronic polarization, allowing the methods to attain computational speeds approaching that of the more approximate additive force fields.

3 Application of polarizable force fields

3.1 Water simulations

Water is an essential component in the chemistry of life, and a high quality water force field is essential for meaningful simulation studies of biological systems. Furthermore, any effort to develop a force field for biomolecular systems must start with a model for water. To meet the need of a computationally tractable yet appropriately accurate model of water an extremely large number of polarizable potentials for water have been developed. These include models based on induced point dipoles [140, 149–167], Drude oscillators [72, 74–77], fluctuating charge models [15, 25, 91, 101, 115, 148, 168, 169] and hybrid induced dipole/fluctuating charge methods [35]. The reader is referred to a previous review on a number of additive and polarizable water models for additional information [16].

Polarizable water models generally perform a good job in reproducing both water dimer interactions energies and enthalpies of vaporization of liquid water, a combination that may be considered a minimum requirement for a model that will be appropriate for a range of environments. Most polarizable water models have dimer interaction energies close to −5.0 kcal/mol, the accepted ab initio value [170]. Examples include −4.69 kcal/mol for the POL3 model [164], −4.51 kcal/mol for the TIP4P-FQ model [91], −5.33 kcal/mol for the model of Burnham et al. [171], −5.00 kcal/mol for the MCDHO model [73], −5.0 kcal/mol for the POL5/TZ model [35] and −5.2 kcal/mol for the SWM4-DP and SWM4-NDP models [76, 77]. For comparison the value of −6.5 kcal/mol for the additive TIP3P is significantly overestimated, as required to obtain accurate pure solvent properties [1].

The ability of polarizable models to accurately treat both the gas phase water dimer energy and bulk water properties allows them to perform better in reproducing the molecular dipoles in environments where the hydrogen bonds network is perturbed [14, 171]. Explicit account of polarization seems essential to accommodate the local disruption of the hydrogen bond network created by anions such as chloride [116, 150, 172, 173] or fluoride [174–178] or to reproduce the polarization effects of small multivalent cations on the first hydration shell [179, 180]. Although explicit polarizability does not appear to have any significant effect on the reorganization of water molecules at liquid-hydrophobic [181] or liquid–vapor [164, 182] interfaces, it may play a decisive role for the specific water–water interactions near small nonpolar moieties [183, 184]. In short, polarizability is essential to obtain accurate energetics in the vicinity of highly polar moieties (such as carbonyl groups), small ions (such as sodium or chloride), and also in anisotropic nonpolar environments.

Liquid phase properties of several polarizable force fields have been studied in great detail, including structural properties (e.g., radial distribution functions, RDF), dielectric constants, and dynamical properties (e.g., diffusion constant and NMR relaxation times). The structure of liquid water is characterized by a short range order and a long-range disorder. This is reflected by the radial distribution function $g(r)$, which can be derived from neutron [185–191] and X-ray [192–196] scattering experiments. Sorenson et al. [197] and Head-Gordon and Hura [198] provide a summary of experimental and simulated atom–atom RDF results. Over the years Soper et al. [185, 190, 199, 200] have reported different results emphasizing the difficulty in unambiguously determining RDFs from experimental scattering data. However, two groups, including results from Soper, have now reported almost identical experimental RDFs based on independent analysis of neutron scattering experiments [190] or X-ray scattering experiments [196], representing the best RDF estimates currently available. It should be noted that the latest structural data reported by Soper [190] is a revised analysis of the experimental data obtained in 1986 [185].

Head-Gordon and Hura [198] compared partial correlation functions of empirical water models such as the nonpolarizable TIP5P model [201], the rigid polarizable model

based on fluctuating charges, TIP4P-pol-1 [115], and a flexible polarizable model based on induced dipoles NCC-vib [202]. The TIP5P five-site additive model is particularly noteworthy given its excellent prediction of the $g_{OO}(r)$ data. The polarizable models also show very good agreement with $g_{OO}(r)$ and, without fitting, often predict the temperature of maximum density of water. None of the models does an outstanding job in reproducing the reanalyzed neutron scattering $g_{OH}(r)$ and $g_{HH}(r)$ data. Sorensen et al. [197] compared experimental radial distribution functions with predictions made for both polarizable and non-polarizable water models. They found that the calculated RDFs for the polarizable models (CC [163], TIP4P-FQ [91]) were generally in better agreement with experiment than those for the additive TIP3P [1] and SPC [203] three-site models. The RDFs for the polarizable force fields, however, were not significantly better than those for the four-site TIP4P model and not as good as those for the additive five-site TIP5P model [201].

Additional polarizable water models were analyzed by Sorenson et al. [197]. They include the fluctuating charge version of TIP4P, TIP4P-FQ [25], an extension of TIP4P that introduces an additional coupling between the Lennard–Jones interaction parameters for the oxygen site and their partial charges [115], TIP4P-Pol-1, an extension of the MCY water model to include flexible bonds and angles, as well as many-body effects, NCC-vib [202], the polarizable point charge model [139], PCC, and a simple polarizable model developed by Chialvo and Cummings to reproduce water properties over a wide range of conditions, CC [163]. The CC model shifts all RDF peaks to larger r, and has a very large peak and shows a loss of density at the first minimum in the RDF. While its structure does least well among the polarizable water models, its reproduces non-ambient states better [163]. The NCC-vib model [202] also overemphasizes the loss of density at the first minimum, but is otherwise good in reproducing the experimentally determined $g_{OO}(r)$. For the TIP4P-FQ model and the PPC models [139], it is evident that the overall agreement is excellent, although the position of the experimental first peak is not as well-reproduced as the nonpolarizable TIP5P model. The TIP4P-pol-1 water model shows improvements in first peak positions relative to TIP4P-FQ, but overemphasizes the loss and gain of density at the first minimum and second maximum, respectively. While the polarizable models perform well overall, many of these models are not as optimal performers at ambient temperature as their nonpolarizable partners. This and their inability to reproduce the RDF as well as the TIP5P model suggests that improved polarizable water models are accessible. Such models may need to include some representation of anisotropic charge distributions (e.g., off-center charges or 'lone pairs'), as well as polarizability.

The ability of models to describe various properties of water in a broad range of thermodynamic states has been accounted to different degrees by the different force fields. The inclusion of the polarizability improves the performance of the water models in various respects. This includes reproduction of the temperature of maximum density [139, 204, 205], and describing the elongation of the hydrogen bonds with increasing temperature [206]. Interestingly polarizable water models proved to be less successful than some of the additive models in reproducing, for instance, the thermodynamic properties of water around the critical point (Table 1) [206]. It has been suggested that better polarizable models may require a different form for the vdW repulsive energy or a more realistic description of polarizability than is possible with a single polarizable atomic center [206]. Another possibility is that molecular flexibility may need to be included in these models. This conjecture is based on the fact that studies have shown that introduction of flexible bond angles (and bond lengths) affects the thermodynamic properties of nonpolarizable models considerably [132, 133, 207–209]. Perhaps, in taking one step forward (inclusion of polarizability) it is necessary to take another (inclusion of flexibility) to yield a more balanced representation of water.

More recent polarizable water models developed for biomolecular simulations are the SWM4-DP and SWM4-NDP model of Lamoureux et al. [76, 77] and the AMOEBA model of Ren and Ponder [45, 46]. The SWM4-DP model is a four-point rigid model, analogous to the TIP4P model, with polarizability described by a Drude oscillator on the oxygen; the SWM4-NDP model is similar to the original SWM4-DP but carries a negative charge on the Drude particle on the oxygen to mimic the electron charge and has different LJ parameters. The RDFs for these

Table 1 Estimates of critical temperature and density of polarizable and nonpolarizable water models

	T_c (K)	ρ_c (Kg m^{-3})
Polarizable models		
TIP4P-FQ [210]	570	300
TIP4P/P [211]	587	350
SPC/P [211]	551	340
SCPDP [211]	538	320
KJ [211]	685	340
PPC [212]	606	300
Nonpolarizable models		
SPC [203]	594	271
SPC/E [213]	639	273
MSPC/E [214]	610	287
Experimental [215]	647	322

models are characterized by the narrow shape of the first peak in the $g_{OO}(r)$ radial distribution and the first intramolecular peak of the $g_{OH}(r)$ distribution is slightly outward ($r_{OH}^{(1)} = 1.85$ Å instead of 1.78 Å). The height of the first peak in the oxygen–oxygen radial distribution function is 3.07, which is somewhat high but almost within the experimental error from the neutron diffraction results ($g_{OO}^{(1)}(r) = 2.7 \pm 0.3$ [216]). Notably, the SWM4 models accurately reproduce the diffusion coefficient and are in satisfactory agreement with experiment for the Debye and NMR relaxation times, indicating their accurate treatment of dynamic properties. These models also accurately reproduce the dielectric constant of water, ε, which is not surprising given that ε was included as target data during optimization of those models. Interestingly, that effort lead to the observation that the gas phase polarizability of water, as well as other molecules, may not be appropriate for the condensed phase. This is consistent with observations based on quantum calculations, as discussed in detail below. While the question of polarizability scaling is still being addressed (see below), it should be emphasized that a proper treatment of the dielectric behavior of water as well as other molecules is important for accurate treatment of solvation energies in different environments and, accordingly, its accurate reproduction by a model may be considered an essential feature.

The AMOEBA water model of Ren and Ponder [45] is fully flexible and was compared with experimental and QM data. Studies of single isolated molecules, molecular clusters, liquid water and ice were performed. AMOEBA calculated dipole and quadrupole moments and polarizability of an isolated water molecule were shown to be in good agreement with experimental and QM results. Tests of the water dimer were also conducted and it was found to be in good agreement with recent theoretical results [217, 218]. Bonding energies and geometries of small water clusters from the trimer to the hexamer were also found to be in good agreement with QM results [219, 220]. Simulations of liquid water were performed and thermodynamic, transport and structural results were compared with experimental data. Of the several quantities computed, density at room temperature and heat of vaporization were in excellent agreement with experimental values, the dielectric constant was slightly higher than the experimental value, the self-diffusion coefficient was lower than the experiment and the viscosity was higher as expected. The structure of liquid water was characterized by computation of O···O, O···H and H···H RDFs sampled from NPT simulations and compared with Soper's 2000 results [190]. It is noteworthy that the experimental curves g_{OO} reported by Soper in 2000 (neutron-diffraction) are almost identical to the ones of Sorensen et al. (X-ray experiments) [197]. The position of the first peak in the $g_{OO}(r)$ radial distribution from the

AMOEBA simulations is 0.08 Å longer and its height is higher than that of the Soper 2000 RDF. The first peaks of the $g_{OH}(r)$ and $g_{HH}(r)$ RDFs are also higher that the Soper 2000 data and the positions of the two peaks are shifted to larger distances. In general, the model provides a credible description of the structural properties of bulk liquid water at room temperature. Studies of two ice forms, ice Ih and XI, were also reported through energy minimization of atomic positions and crystal lattices and MD simulations. The computed results are in very good agreement with the experimental data. The same authors published another study where the temperature and pressure dependence of the AMOEBA water model are analyzed [46].

3.2 Ion solvation

One of the most critical needs for a biological polarizable force field is the treatment of both atomic and molecular ions. Ion solvation is important in chemistry, including surface chemistry, environmental chemistry, and the study of molecules such as surfactants, colloids, and polyelectrolytes. Biologically, ions are critical to the structure and function of nucleic acids, proteins, and lipid membranes and ion transport in and out of the cell plays a central role in numerous physiological processes [221–225]. The structure of nucleic acids is affected by nonspecific counterion condensation [226] as well as specific interactions [227, 228]. Ion binding to specific protein sites occurs for purposes of stabilization as well as playing central roles in enzyme catalysis [229–231]. Ion permeation across the cell membrane is tightly controlled by specialized proteins called ion channels [232–234]. In physical chemistry, ion solvation is also important in several processes such as chemical purification [235] and chromatographic systems [236] and ion-specific chelators [237].

Simulations of aqueous ionic solutions using nonpolarizable additive force fields have shown that consideration of non-additive effects is important to accurately reproduce the atomic details of ion hydration [43, 116, 150, 173, 238–240]. In principle, accurate potential functions for computer simulations can be developed and validated by comparing to experimental data (gas phase and bulk) and to the results of high level QM ab initio computations performed on ion–water dimers and small ion-solvent clusters [43, 79]. Experimental target data available to parametrize and validate MM models of ion–water systems include gas phase energies of small hydrated clusters [241], bulk hydration free energies [242, 243], structural properties (radial distribution function, coordination numbers, etc.), and transport coefficients (diffusion constant, mobility, conductivity). Åqvist was the first to develop additive ion–water interaction potentials for the most common ions in biology using calculations of the absolute hydration free

energy in bulk water [244]. The models were constructed for the nonpolarizable SPC water model, but have also been translated for the TIP3P and TIP4P model, giving rise to a number of unanticipated issues (see recent article by Cheatham [245]). A similar route was taken to develop an independent set of ions for the TIP3P model [246, 247].

Correct interpretation of the experimental hydration free energies of ions and its use in constructing an accurate computational model is, in fact, not as straightforward as one would wish [78, 79]. One difficulty arises because experimental thermodynamic or electrochemical measurements involve neutral macroscopic systems and have access only to irreducible, *conventional* hydration free energies that are either the sum of the absolute free energies of an ion and a counterion, $\Delta G_{\text{hyd}}(M^+) + \Delta G_{\text{hyd}}(X^-)$, or the difference of the free energies of two ionic species of the same valence, $\Delta G_{\text{hyd}}(M_1^+) + \Delta G_{\text{hyd}}(M_2^+)$. In fact, the absolute hydration free energy of a single ion cannot be resolved from calorimetric or electrochemical experiments alone. So, while the solvation free energy for a neutral salt can be measured, it is impossible to separate it experimentally into contributions from the cation and anion [242, 248, 249]. An additional extrathermodynamic assumption is required to perform this dissection [250]. A detailed explanation of the pros and cons of the different methods can be found in Ref. [43] and in [78]. In the same references, alternative methods were proposed to deal with this assumption. Lamoureux and Roux examined the sensitivity of the bulk hydration free energy of individual ions to the gas phase monohydrate energy and showed that the absolute scale varies only within a narrow range. The implication is that the gas phase monohydrate energies puts, by itself, a tight constraint on the absolute scale of hydration free energies of ions. This analysis was used to set the absolute scale of hydration free energy and develop a consistent parametrization for the complete alkali-halide series. This type of analysis, relating monohydrate and bulk solvation properties, goes back to the pioneering study of Åqvist [244].

Several studies of the solvation of ions and salts have been published using the different polarizable models implemented in CHARMM. Lamoureux and Roux developed polarizable potential functions for the hydration of alkali and halide ions using the SWM4-DP water model. Patel and co-workers published several studies of solvation of ions and salts in water using the polarizable TIP4P-FQ water model implemented in CHARMM [251–253]. In another study from that laboratory [251] the TIP4P-FQ model was compared with the additive TIP4P and the Drude water models. Roux and co-workers have presented a study of aqueous solvation of K^+ and compared ab initio, polarizable (SWM4-NDP Drude water model of CHARMM) and additive force field methods [79]. All

computational methods yielded hydration numbers between 5.9 (Car-Parrinello PW91/pw) and 6.8 (Drude model) in good agreement with experimental data (6–7).

Other authors have presented studies relevant to understand the performance of electronic polarization in interactions of molecules with ions. Masia and co-workers [254] studied the interaction of a molecule with a cation, via induced dipoles and Drude oscillators. The dimer electric dipole moments as a function of the ion-molecule distance for selected molecular orientations was compared with high-level ab initio calculations for water or carbon tetrachloride close to Li^+, Na^+, Mg^{2+}, and Ca^{2+}. It was shown that the simple polarization methods are able to satisfactorily reproduce the induced dipole moment of the cation-molecule dimer. In a previous study, the same authors studied the interactions between molecules and point charges [255].

A potential model for Li^+-water clusters was presented [256] and the same authors performed a detailed study of the monovalent ions, Li^+, Na^+, K^+, F^-, Cl^-, and Br^- in aqueous solution and the small water clusters $M^+(H_2O)_n$ and $M^-(H_2O)_n$. These studies were based on the ABEEM/MM method. Analysis of results from these studies included solvation structures, charge distributions, binding energies, dynamic properties (diffusion coefficients of ions) and free energies of hydration [257]. The computed quantities were found to be in good agreement with experimental results.

A study of solvation dynamics of divalent cations in water was performed by Piquemal et al. [258] using a modified AMOEBA force field. The model consisted of a cation specific parametrization based on ab initio polarization energies computed by a constrained space orbital variation (CSOV) energy decomposition method [259]. Excellent agreement between computed and experimental condensed phase properties was found despite the use of parameters derived from gas phase ab initio calculations.

A number of studies of the influence of ions on the air–water interface using polarizable models have been published. A useful review of these studies is that by Jungwirth and Tobias [260]. Examples include the study of Salvador et al. of the aqueous solvation of NO_3^- in interfacial environments with a Car-Parrinello MD simulation of a cluster and classical MD of an extended slab system with bulk interfaces using a polarizable force field based on the atoms in molecules analysis (AIM) [261]. Both in aqueous clusters and in systems with extended interfaces the nitrate anion clearly prefers interfacial over bulk solvation. Archontis and co-workers studied the distribution of iodine at the air–water interface using the Drude based SWM4-DP water model [262, 263] and Jungwirth and co-workers performed similar studies using the AMOEBA force field [264]. In all cases it was found that iodine tends to remain

closer to the water/vapor and that tendency to stay at the interface increases in the order $Cl^- < Br^- < I^-$. More recently, studies of several ions and salts at the air–water interface have been published. Tobias and co-workers have presented a mixed X-ray photoemission spectroscopy/MD study using polarizable potentials of aqueous potassium fluoride solutions [265]. Wang et al. studied NaCl using a Drude model [266] and Warren and Patel compared several polarizable ion models [252, 253]. MD studies of aqueous solutions of molecular ions have also been published. Picalek et al. [267] studied the interfacial structure of aqueous solutions of 1-butyl-3-methylimidazolium tetrafluoroborate and 1-butyl-3-methylimidazolium hexafluorophosphate using both non-polarizable and polarizable force fields.

Specialized uses of combined QM and MD methods have been presented. Roos and co-workers [268] studied the coordination environment of the uranyl ion in water. Pair potentials were initially calculated using multiconfigurational wave function calculations and the quantum chemically determined energies were used to fit parameters in a polarizable force field with an additional charge transfer term. Classical MD simulations were performed for the uranyl ion and up to 400 water molecules. The results show a uranyl ion with five water molecules coordinated in the equatorial plane. The U-$O(H_2O)$ distance is 2.40 Å and a second coordination shell starts at about 4.7 Å from the uranium atom. Interestingly, no hydrogen bonding is found between the uranyl oxygens and water.

In summary, polarizable force fields have been shown to be very promising for simulating the properties of ionic systems. Particularly satisfying, though not surprising, is their ability to successfully describe interfacial systems more accurately than additive models. This further emphasizes the importance of the ability of polarizable models to accurately treat environments of varying polarity to produce a more accurate representation of the experimental regimen.

3.3 Application of polarizable models to small molecules

A number of small molecules have been studied using polarizable force fields. Examples include the major organic functional groups, for example, pure alkanes, alcohols, thiols, aromatic compounds, aldehydes, ketones, ethers, amines and amides; chlorinated compounds, including CCl_4 and CH_2Cl_2, and the guanidinium ion. Many studies included the compounds in aqueous solution.

Early studies of small organic molecules were limited to determination of electrostatic properties using polarizable methods. No et al. applied an electronegativity equalization method to determine net atomic charges of 25 small

organic molecules including alcohols, ethers, esters, aldehydes, ketones, thiols, thioethers, secondary amines and alkanes [269], and to ionic and aromatic compounds [270].

An early condensed phase study of polarizable alkanes was presented by Rick and Berne [184]. The manuscript reported the free energy of methane association in water using a polarizable fluctuating charge model. Two previous studies only included polarizability on the water molecules [183, 271]. The hydrophobic interaction was more recently analyzed using polarizable models by Rick [272], who calculated the heat capacity change for methane pair aggregation. Chelli and co-workers [126] applied the fluctuating point charge model (FQ) and the atom–atom charge transfer model (AACT), fitted to the polarizability of small alkanes and polyenes, to larger homologues. The AACT scheme was found to perform better on alkanes of any length and conformation. The AACT scheme also satisfactorily reproduced the polarization response for highly conjugated systems.

A number of additional studies of alkanes using polarizable models have been reported. Bret et al. developed force field parameters for methane in the framework of the chemical potential equalization model [97]. Studies of methane clathrate hydrates were performed by English and MacElroy [273] using flexible and rigid polarizable and nonpolarizable water and flexible and rigid methane models. Parametrization and testing of the ABEEM/MM fluctuating charge force field for alkanes was described by Zhang and Yang [274]. Borodin and Smith [275] reported the development of many-body polarizable force fields for ether, alkane and carbonate-based solvents. Alkane parameters were also developed for the polarizable methods included in CHARMM. MacKerell and co-workers presented a systematic study of a Drude oscillator-based model of alkanes [85], calculating bulk thermodynamic, structural, dielectric, and aqueous solvation properties. Patel and Brooks [276] presented a study on a polarizable model of hexane in the framework of the fluctuating charge method, focusing on bulk liquid phase properties and analysis of the hexane–water interface. Recently, this work was extended to include longer alkanes by Davis et al. [277]. Development of a polarizable intermolecular potential function (PIPF) for liquid amides and alkanes has been reported [36]. Another application reported by Jalkanen and Zerbetto [278] studied the adsorption of organics on a silver surface using an embedded atom model for the metal, a standard bonded potentials for the organics, and a combination of the charge equilibration model and the Morse potential for their electrostatic and nonbonding interactions.

Alcohols were the subject of several studies using polarizable force fields. One of the earliest studies of a nonadditive MD simulation of a pure alcohol was reported

by Caldwell and Kollman, who studied the structure and properties of pure methanol [279]. This was followed by calculation of the aqueous solution free energy of methanol [280]. Chelli and co-workers applied the chemical potential equalization method to calculate the optical spectra of liquid methanol [96, 98] and investigated the polarization response of methanol by polarizable force field and density functional theory calculations [281]. The method to model polarization developed by Ferenczy and Reynolds [282, 283] was also applied to methanol complexes [284]. Methanol was also used in the development of the induced dipole method of Berne, Friesner and co-workers [285]. A polarizable model for simulation of liquid methanol was developed using the Charge-on-Spring (COS) technique and is compatible with the COS/G2 water model. The model was used to study the thermodynamic, dynamic, structural, and dielectric properties of liquid methanol and of a methanol–water mixture [286]. MC simulations of liquid methanol have also been reported using a potential including polarizability, nonadditivity, and intramolecular relaxation [287]. The classical Drude oscillator model implemented in CHARMM was used to study water–ethanol mixtures by Noskov et al. [68]. Interestingly, although the water and ethanol models were parametrized separately to reproduce their respective vaporization enthalpies, static dielectric constants, and self-diffusion constants of the pure liquids, the model was able to reproduce the energetic and dynamical properties of the mixtures accurately. Furthermore, the calculated dielectric constant for the various water–alcohol mixtures is in excellent agreement with experimental data. A revised Drude model for primary and secondary alcohols has been presented by Anisimov et al. [69]. That work indicated significant differences in alcohol–water RDFs as compared to the CHARMM additive force field, suggesting that the inclusion of polarizability alters atomic details of the interactions between these classes of molecule. Parameters for ethanol and methanol have also been developed for the FQ implementation in CHARMM [288, 289]. Recently, thermodynamic and structural properties of methanol–water solutions were published using that model [290]. Polarizable force fields have also been developed for thiols and other sulfur containing compounds like thioethers and disulfides. Noteworthy is the work of Kaminski et al. [285, 291] and sulfur parameters based on the Drude oscillator model are in progress (X. Zhu and A.D. MacKerell, Jr., Work in progress).

Other classes of small organic molecules studied with polarizable force fields are aromatic and heteroaromatic compounds. Stern et al. parameterized electrostatic parameters of substituted benzenes based on fluctuating charge, induced dipole, and a combined model and applied the resulting parameters to compute conformational energies of the alanine, serine and phenylalanine dipeptides [87]. The effort of Berne, Friesner and co-workers to develop a polarizable force field for small organic molecules within a fluctuating charge approach also included benzene and phenol [291]. The development of the DRF90 force field of Swart and van Duijnen relied on comparison of computed interaction energies and geometries of benzene dimers with ab initio results [29]. Lopes et al. published a study of aromatic compounds using the classical Drude formalism implemented in CHARMM. Benzene dimer interaction energies and geometries were considered and thermodynamic and transport properties in condensed phase were computed and compared with experimental values [70]. Soteras et al. developed models of distributed atomic polarizabilities for the treatment of induction effects in MM simulations within the framework of the induced dipole model. Molecular polarizabilities were computed for benzene, pyridine, imidazole, indole, aniline, benzonitrile, phenol and halogenated benzenes [292]. Mayer and Astrand developed a charge-dipole model for the static polarizability of nanostructures that include aliphatic, olephinic and aromatic systems [293]. MacKerell and co-workers have recently published force field parameters for pyridine, pyrimidine, imidazole, pyrrole, indole and purine [10], an effort that will lay the ground work for the development of a nucleic acids force field. That effort relied heavily on the reproduction of a variety of experimental condensed phase properties including pure solvents, crystals and aqueous solvation. Use of multiple types of condensed phase data is important is it increases the number of types of molecules that can be optimized using experimental thermodynamic data and the types of environments that can be considered during the force field optimization.

Ethers, ketones and aldehydes are among the most studied molecules using polarizable force field methods. Shirts and Stolworthy [294] analysis of a crown ether (18-crown-6) showed that the electrostatic term is the largest contributor to the conformational energy and discussed the desirability of using a polarizable method, such as the charge equilibration algorithms, to include these effects in MM and MD calculations. During development of the FQ method by Berne and co-workers investigations of the aqueous solvation and reoganization energy of other molecules, notably formaldehyde, were performed [295, 296]. The development of new schemes of including polarization in classical force fields often used water-formaldehyde complexes as a source of target data for the parametrization. The methods to model polarization developed by Ferenczy and Reynolds [282, 283] and Krimm and co-workers included formaldehyde–water complexes [284, 297]. Borodin and Smith developed classical polarizable force fields for several molecules including polyethers,

ketones, and linear and cyclic carbonates on the basis of QM dimer energies of model compounds and empirical thermodynamic liquid-state properties [275, 298–304].

The first studies of amines and amides using polarizable force fields were the hydration calculations by Kroghjespersen et al. [305], and of amine hydration by Kollman and co-workers [306]. Despite the very different parametrizations, inclusion of polarizability substantially improved the reproduction of the experimental free energies of aqueous solvation in both studies. Amides, in particular N-methylacetamide (NMA), are extremely important in the development of polarizable force fields for proteins since they constitute the smallest unit representative of the polypeptide backbone. Recently, MacKerell, Roux and co-workers parametrization of NMA within the context of the classical Drude polarizable method was the first force field to reproduce the large dielectric constant of liquid NMA [84]. Polarizable models of amide compounds that have two (acetamide) and zero (N,N-dimethyl acetamide) polar hydrogen-bond donor atoms were also investigated. In those studies it was shown that a proper representation of both the magnitude and direction of the molecular polarizability tensor, made possible by the use of atom-based Thole damping factors, was essential to obtain the correct dielectric response.

The ability of polarizable force fields to accurately reproduce dielectric constants deserves additional discussion. Although the dielectric is a macroscopic property of bulk system, it has a critical impact on microscopic interactions within the system. This can be qualitatively illustrated by considering the familiar Born model of solvation, which shows that the solvation free energy of an ion of charge q and radius R is given by $q^2/(2R)$ $(1/\varepsilon - 1)$. This expression shows that correct estimation of ε is essential to obtain the proper solvation thermodynamics. The treatment of induced electronic polarization becomes of particular importance in the case of the low-dielectric alkanes. The correct value of ε is approximately 2, which is only possible to attain in polarizable models as additive models with fixed partial charges yield values that are approximately equal to 1 [85]. Obviously, going from a value of 1 to 2 drastically impacts solvation energies, as shown in the context of the Born approximation, such that the ability of force fields to model relative solvation in complex simulations, such as lipid bilayers, will be drastically effected. For example, the neglect of polarization of the hydrocarbon core of lipid membranes has been shown to have great practical consequences in computational studies of ion channels [307, 308]. However, attaining the correct dielectric behavior appears to not be trivial. In our own hands, the assumption that the gas phase polarizabilities would be applicable to the condensed phase was shown to be incorrect on the first molecule studied, water, as

discussed above. This lead to the development of an approach whereby the polarizability of a molecule is considered a free parameter during optimization, with the primary target data being reproduction of the dielectric constant of the corresponding pure solvent. To date, our efforts indicate that the appropriate polarizability depends on the class of molecule under study. As quantified in terms of scaling of the gas phase polarizability, we have empirically determined scaling factors ranging from 0.7 for water, alcohols and sulfur containing species, 0.85 for aromatics, N-containing heteroaromatics and ethers (C. Baker and A.D. MacKerell, Jr. Work in progress) and 1.0 for amides. Given the role of electrostatics in a variety of complex phenomena involving biological systems (e.g., pK$_a$s, reduction potentials) and the contribution of the dielectric to proper treatment of electrostatics, careful consideration of this important term is central to successful development of polarizable force fields for biological molecules.

QM studies also indicate that polarizability scaling for the condensed phase may be necessary. Based on studies of water clusters, it was suggested that in the condensed phase, polarization is lower than in gas phase because of the energetic cost arising from Pauli's exclusion principle due to the overlap of neighbouring electronic charge distributions [309]. A recent study by Schropp and Tavan [310] on the polarization of a single QM water molecule within a MM described bulk phase also concluded that the gas phase experimental polarizability cannot be used in molecular simulations but must be reduced to an effective polarizability. It was argued that in the liquid phase the electric field, $\langle \mathbf{E} \rangle$, in the excluded volume of each water molecule is strongly inhomogeneous such that the electric field at the position of the oxygen (or hydrogens), $\mathbf{E}(\mathbf{r}_O)$, is not appropriate for calculation of the molecular polarizability. Since $\langle \mathbf{E} \rangle$ is smaller than $\mathbf{E}(\mathbf{r}_O)$ and it is necessary to use $\mathbf{E}(\mathbf{r}_O)$ in MD simulations because of computational efficiency, results that $\mathbf{E}(\mathbf{r}_O)$ needs to be scaled to match $\langle \mathbf{E} \rangle$. Remarkably, the scaling factor proposed by Schropp and Tavan (0.68) is close to the empirical value of approximately 0.7 proposed by Lamoureux et al. [76, 77]. Another recent study using semiempirical methods on model compounds representative of phospholipids also indicated that the polarizability of the head group decreased in the presence of water, suggesting the effect is due to making "electrons in hydrogen bonds to be more bound" [311]. However, the AMEOBA water model, which has been developed with inducible point-dipoles on the oxygen as well as on the hydrogen atoms without any scaling, only slightly overestimates the dielectric of bulk water under ambient conditions (see above), indicating that the extent of scaling may also be dependent on the method used to treat polarizability. Thus, while both QM as well as

empirical approaches based on reproduction of condensed phase properties indicate the need for polarizability scaling for some classes of molecules, the cause of the effect is still a matter of debate.

In general, the simulation studies of small molecules using polarizable models have shown that the extension of empirical force fields to include polarization is indeed feasible. In many, but not all cases the polarizable models have lead to improved agreement with experiment. In addition, the atomic details of the interactions between components in condensed phase simulations have been observed to differ in polarizable models as compared to additive models [70, 85]. Thus, it appears that polarizable models will lead to a more accurate picture of the atomic details of condensed phases; however, it should emphasized that careful optimization methods, including optimization of the LJ parameters, followed by rigorous validation of the models is essential to assure that those models are yielding atomic pictures representative of the experimental regimen.

3.4 Application of polarizable force fields to proteins, nucleic acids and lipid bilayers

The ultimate goal of polarizable force fields with biological relevance is the development of fully usable, high quality force fields applicable to simulations of large biomolecules: proteins, DNA/RNA, lipid bilayers and carbohydrates. While the development of such force fields that have been fully optimized is still in its infancy, very early studies that applied polarizable models to proteins in MM calculations should be noted. These include a study of lysozyme by Warshel and Levitt [312] who simulated the electrostatic environment by a polarizable force field based on induced dipoles and represented the effect of the surrounding solvent by a microscopic dielectric model. Similar approaches were used for other systems [138, 313, 314]. While these studies only involved single point calculations (i.e. calculation of the polarization response on a single protein conformation), they emphasize that early workers were well aware of the importance of this term in theoretical studies of macromolecules. And given that it has taken over 25 years since those seminal works to start to systematically apply polarizable models to macromolecules, it is clear that the technical hurdles to the implementation and development of polarizable models have and will continue to be large. Only recently has there was a surge of publications on large molecules indicating that many of the polarizable force fields being developed in the past 10 years are nearing completion [315]. At the time of writing, many studies are still focused on validating the various force fields that have been developed over the years. However, fully featured studies that address specific research have already been published.

One of the first modern applications of a polarizable force field to a protein was on crambin using the fluctuating charge method interfaced with the UFF and AMBER force fields [111]. The polarizable charges were found to give more realistic charge redistribution between amino acids in the protein. Berne and co-workers used a combination of permanent and inducible point dipoles with fluctuating and fixed charges to simulate bovine pancreatic trypsin inhibitor (BPTI) in water with two commonly used water models TlP4P-FQ and RPOL. The simulated structures remain within 1 Å of the experimental crystal structure for the 2 ns duration of the simulations [316, 317]. The extent of deviation of the structure was similar to that obtain with the OPLS all-atom additive force field. More recently, Liang and Walsh studied aqueous solvation of carboxylate groups present in the glycine zwitterion and the dipeptide aspartylalanine using the AMOEBA force field. Results were compared with Car-Parrinello MD data and additive force fields. The polarizable force field yields carboxylate solvation properties in very good agreement with CPMD results, agreement that was significantly closer than that obtained from traditional force fields [318].

Llinas et al. performed structural studies of human alkaline phosphatase using the TCPEp (topological and classical polarization effects for proteins) force field [319]. The enzyme possesses 4 metal binding sites, two for Zn^{2+}, one for Mg^{2+} and one Ca^{2+}. In this study, Ca^{2+} was replaced by Sr^{2+}, both showing similar interaction energies at the calcium-binding site. Only at high doses of strontium, comparable to those found for calcium, can strontium substitute for calcium. Since osteomalacia is observed after ingestion of high doses of strontium, alkaline phosphatase is likely to be one of the targets of strontium, and thus the results support the suggestion that the enzyme may be involved in this disease.

In a step forward towards a polarizable force field for proteins Wang et al. optimized the the AMBER polarizable model parameters adjusting the phi and psi torsion angles of the protein backbone by fitting to the QM energies of the important regions: beta, P-II, alpha(R), and alpha(L) regions [320]. Performance of the force field was analysed by comparison of energies against QM data and by the replica exchange molecular dynamics simulations of short polyalanine peptides in water. The populations in these three regions were found to be in qualitative agreement with the NMR and CD experimental results.

The ABEEM/MM method has been tested in studies of peptides and proteins. The first of those studies is a conformational analysis of a peptide in 2006 [321], followed by studies of trypsin inhibitors [322], BPTI in aqueous solution and conformational studies of alpha-conotoxin GI [323]. A study on the geometry of the heme prosthetic group was also published in 2008 [324].

Extension of polarizable force fields to studies of other classes of biomolecules has also been published. Allen and co-workers compared newly developed coarse-grained models, with the additive CHARMM27 force field and the newly developed Drude force field on the energetics of membrane–arginine interactions [325]. An innovative application of polarizable force fields was presented by Masella and co-workers, who combined a polarizable force field and a coarse-grained polarizable solvent with application to a long simulation of bovine pancreatic trypsin inhibitor [326]. The method was found to be much faster than traditional approaches where solvent is treated atomistically. Specialized applications included application of a polarizable force field to calculation of protein-ligand binding energies [327] and calculation of the infrared spectra of the polypeptide backbone [328].

The first application of polarizability to an MD simulation of DNA using the Drude oscillator model was performed by MacKerell and co-workers [82] in combination with the CHARMM27 all-atom nucleic acid force field [34]. The system included a DNA octamer and a full solvent representation based on the SWM4-DP model with sodium counterions. The simulation system was shown to be stable, ultimately for 5 ns, though the RMS difference with respect to canonical B form DNA continually increased, well beyond that of a simulation using the CHARMM27 additive model. This deviation emphasizes the importance of full optimization of a force field when the electrostatic model is changed. This is due to the electronic term affecting geometries, vibrations and conformational energies as well as interactions with the environment. More recently, Sagui and co-workers performed molecular dynamics simulations of a DNA decamer using both additive atomic point charge and polarizable force fields [329–331]. Results showed the polarizable model to yield properties similar to that of the additive FF, which may be associated with the underpolarization of the induced dipole model used in that study.

An updated overview of current DNA modeling with ab initio (Hartree-Fock, density functional theory, and tight binding approximations) and empirical methods including polarizable methods has been published by Cozmuta and Mehrez [332]. The authors extensively review the literature until 2007. Another interesting review worth mentioning discusses the merits and limitations of modeling methods available for guanine quadruplex (G-DNA) molecules [333, 334]. Although not focused on polarizable force fields it is an important source of information for the computational chemist/biologist working in the field. The review discusses the relation of simulation results to experimental techniques and the significance of those relationships. Aspects such as: pair-additive approximation of the empirical force fields, sampling limitations due to limited simulation times, accuracy of description of base stacking, H-bonding, sugar-phosphate backbone and ions by force fields, are addressed.

4 Summary

Empirical force fields that explicitly treat electronic polarizability have been known for over 30 years. However, due to technical challenges associated with their implementation, difficulties in the optimization of sufficiently accurate models, and computational demands it is only in recent years that they have started to be increasingly considered. Over the last 15 years a large number of studies using polarizable models of water, ions and of small molecules have been published. The most notable insights from these efforts are in the area of ion solvation and at interfaces and it is evident that atomistic details of intermolecular interactions differ between polarizable and additive force fields. With respect to macromolecules, a number of works have been published over the last several years with emphasis on the capabilities and accuracy of polarizable models, particularly of proteins. While the application of polarizable models to macromolecular systems has been slow to get out of the gate, it is clear that over the next decade highly optimized polarizable force fields for these systems will become available and widely used. We eagerly look forward to the novel insights that will be obtained from these studies.

References

1. Jorgensen WL, Chandrasekhar J, Madura JD et al (1983) J Chem Phys 79:926
2. Cornell WD, Cieplak P, Bayly CI et al (1995) J Am Chem Soc 117:5179
3. MacKerell AD, Bashford D, Bellott M et al (1998) J Phys Chem B 102:3586
4. MacKerell AD Jr, Brooks B, Brooks CLIII et al (1998) In: Schleyer PVR et al (eds) Encyclopedia of computational chemistry. John Wiley & Sons, Chichester
5. Scott WRP, Hunenberger PH, Tironi IG et al (1999) J Phys Chem A 103:3596
6. Jorgensen WL, Tiradorives J (1988) J Am Chem Soc 110:1657
7. Halgren TA, Damm W (2001) Curr Opin Struct Biol 11:236
8. Rick SW, Stuart SJ (2002) In: Lipkowitz KB, Boyd DB (eds) Reviews in computational chemistry. Wiley-VCH, Hoboken, NJ
9. Warshel A, Kato M, Pisliakov AV (2007) J Chem Theor Comput 3:2034
10. Lopes PEM, Lamoureux G, MacKerell AD (2009) J Comp Chem 30:1821
11. Bayly CI, Cieplak P, Cornell WD et al (1993) J Phys Chem 97:10269
12. Mackerell AD (2004) J Comp Chem 25:1584

13. Dyke TR, Muenter JS (1973) J Chem Phys 59:3125
14. Gregory JK, Clary DC, Liu K et al (1997) Science 275:814
15. Sprik M (1991) J Phys Chem 95:2283
16. Wallqvist A, Mountain R (1999) In: Lipkowitz KB, Boyd DB (eds) Reviews in computational chemistry. Wiley-VCH, New York
17. Soetens JC, Costa M, Millot C (1998) Mol Phys 94:577
18. Silvestrelli PL, Parrinello M (1999) J Chem Phys 111:3572
19. Silvestrelli PL, Parrinello M (1999) Phys Rev Lett 82:3308
20. Silvestrelli PL, Parrinello M (1999) Phys Rev Lett 82:5415
21. Badyal YS, Saboungi ML, Price DL et al (2000) J Chem Phys 112:9206
22. Gubskaya AV, Kusalik PG (2002) J Chem Phys 117:5290
23. Kuo IF, Tobias DJ (2001) J Phys Chem B 105:5827
24. Jorgensen WL (2007) J Chem Theory Comp 3:1877
25. Liu YP, Kim K, Berne BJ et al (1998) J Chem Phys 108:4739
26. Maple JR, Cao YX, Damm WG et al (2005) J Chem Theor Comput 1:694
27. Patel S, Brooks CL (2004) J Comp Chem 25:1
28. Patel S, Mackerell AD, Brooks CL (2004) J Comp Chem 25:1504
29. Swart M, van Duijnen PT (2006) Mol Simul 32:471
30. Ma BY, Lii JH, Allinger NL (2000) J Comp Chem 21:813
31. Thole BT (1981) Chem Phys 59:341
32. Applequist J, Carl JR, Fung K-K (1972) J Am Chem Soc 94:2952
33. Kuyper LF, Hunter RN, Ashton D et al (1991) J Phys Chem 95:6661
34. Foloppe N, MacKerell AD (2000) J Comp Chem 21:86
35. Stern HA, Rittner F, Berne BJ et al (2001) J Chem Phys 115:2237
36. Xie WS, Pu JZ, MacKerell AD, Gao J (2007) J Chem Theor Comput 3:1878
37. Gao JL, Habibollazadeh D, Shao L (1995) J Phys Chem 99:16460
38. Gao JL, Pavelites JJ, Habibollazadeh D (1996) J Phys Chem 100:2689
39. van Duijnen PT, Swart M (1998) J Phys Chem A 102:2399
40. Xie W, Pu J, Gao J (2009) J Phys Chem A 113:2109
41. Ferenczy GG, Reynolds CA (2001) J Phys Chem A 105:11470
42. Ren PY, Ponder JW (2002) J Comp Chem 23:1497
43. Grossfield A, Ren PY, Ponder JW (2003) J Am Chem Soc 125:15671
44. Grossfield A, Ren PY, Ponder JW (2003) Biophys J 84:94A
45. Ren PY, Ponder JW (2003) J Phys Chem B 107:5933
46. Ren PY, Ponder JW (2004) J Phys Chem B 108:13427
47. Grossfield A (2005) J Chem Phys 122:024506
48. Jiao D, King C, Grossfield A et al (2006) J Phys Chem B 110:18553
49. Rasmussen TD, Ren PY, Ponder JW et al (2007) Int J Quantum Chem 107:1390
50. Drude P (1902) The theory of optics. Kessinger Publishing Company, MT (2008)
51. London F (1937) Trans Faraday Soc 33:8b
52. Bade WL (1957) J Chem Phys 27:1280
53. Bade WL, Kirkwood JG (1957) J Chem Phys 27:1284
54. Bade WL (1958) J Chem Phys 28:282
55. Whitfield TW, Martyna GJ (2006) Chem Phys Lett 424:409
56. Amos AT (1996) Int J Quantum Chem 60:67
57. Wang F, Jordan KD (2002) J Chem Phys 116:6973
58. Dick BG, Overhauser AW (1958) Phys Rev 112:90
59. Hanlon JE, Lawson AW (1959) Phys Rev 113:472
60. Jacucci G, McDonald IR, Singer K (1974) Phys Lett A 50:141
61. Lindan PJD, Gillan MJ (1993) J Phys: Condens Matter 5:1019
62. Mitchell PJ, Fincham D (1993) J Phys: Condens Matter 5:1031
63. Lindan PJD (1995) Mol Simul 14:303
64. Hoye JS, Stell G (1980) J Chem Phys 73:461
65. Pratt LR (1980) Mol Phys 40:347
66. Lado F (1997) J Chem Phys 106:4707
67. Cao J, Berne BJ (1993) J Chem Phys 99:2213
68. Noskov SY, Lamoureux G, Roux B (2005) J Phys Chem B 109:6705
69. Anisimov VM, Vorobyov IV, Roux B et al (2007) J Chem Theor Comput 3:1927
70. Lopes PEM, Lamoureux G, Roux B et al (2007) J Phys Chem B 111:2873
71. Saint-Martin H, Medina-Llanos C, Ortega-Blake I (1990) J Chem Phys 93:6448
72. de Leeuw NH, Parker SC (1998) Phys Rev B 58:13901
73. Saint-Martin H, Hernandez-Cobos J, Bernal-Uruchurtu MI et al (2000) J Chem Phys 113:10899
74. van Maaren PJ, van der Spoel D (2001) J Phys Chem B 105:2618
75. Yu HB, Hansson T, van Gunsteren WF (2003) J Chem Phys 118:221
76. Lamoureux G, MacKerell AD, Roux B (2003) J Chem Phys 119:5185
77. Lamoureux G, Harder E, Vorobyov IV et al (2006) Chem Phys Lett 418:245
78. Lamoureux G, Roux B (2006) J Phys Chem B 110:3308
79. Whitfield TW, Varma S, Harder E et al (2007) J Chem Theor Comput 3:2068
80. Lu ZY, Zhang YK (2008) J Chem Theor Comput 4:1237
81. Lamoureux G, Roux B (2003) J Chem Phys 119:3025
82. Anisimov VM, Lamoureux G, Vorobyov IV et al (2005) J Chem Theor Comput 1:153
83. Harder E, Anisimov VM, Vorobyov IV et al (2006) J Chem Theor Comput 2:1587
84. Harder E, Anisimov VM, Whitfield TW et al (2008) J Phys Chem B 112:3509
85. Vorobyov IV, Anisimov VM, MacKerell AD (2005) J Phys Chem B 109:18988
86. Vorobyov I, Anisimov VM, Greene S et al (2007) J Chem Theor Comput 3:1120
87. Stern HA, Kaminski GA, Banks JL et al (1999) J Phys Chem B 103:4730
88. Banks JL, Kaminski GA, Zhou RH et al (1999) J Chem Phys 110:741
89. Kaminski GA, Stern HA, Berne BJ et al (2002) J Comp Chem 23:1515
90. Yin DX, Mackerell AD (1998) J Comp Chem 19:334
91. Rick SW, Stuart SJ, Berne BJ (1994) J Chem Phys 101:6141
92. Nalewajski RF (1991) Int J Quantum Chem 40:265
93. Chelli R, Procacci P (2002) J Chem Phys 117:9175
94. Itskowitz P, Berkowitz ML (1997) J Phys Chem A 101:5687
95. Nalewajski RF (1998) Pol J Chem 72:1763
96. Chelli R, Ciabatti S, Cardini G et al (1999) J Chem Phys 111:4218
97. Bret C, Field MJ, Hemmingsen L (2000) Mol Phys 98:751
98. Chelli R, Ciabatti S, Cardini G et al (2000) J Chem Phys 112:5515
99. Nalewajski RF (2000) Int J Quantum Chem 78:168
100. Llanta E, Ando K, Rey R (2001) J Phys Chem B 105:7783
101. York DM, Yang WT (1996) J Chem Phys 104:159
102. Smith PE (2004) J Phys Chem B 108:16271
103. Chelli R, Barducci A, Bellucci L et al (2005) J Chem Phys 123:194109
104. Medeiros M (2005) Theor Chem Acc 113:178
105. Piquemal JP, Chelli R, Procacci P et al (2007) J Phys Chem A 111:8170
106. Warren GL, Davis JE, Patel S (2008) J Chem Phys 128:144110
107. Zhang Y, Lin H (2008) J Chem Theor Comput 4:414

108. Rappé AK, Goddard WA (1991) J Phys Chem 95:3358
109. Kitao O, Ogawa T (2003) Mol Phys 101:3
110. Nistor RA, Polihronov JG, Muser MH et al (2006) J Chem Phys 125:094108
111. Ogawa T, Kurita N, Sekino H et al (2004) Chem Phys Lett 397:382
112. Sefcik J, Demiralp E, Cagin T et al (2002) J Comp Chem 23:1507
113. Tanaka M, Siehl HU (2008) Chem Phys Lett 457:263
114. Brodersen S, Wilke S, Leusen FJJ et al (2005) Cryst Growth Des 5:925
115. Chen B, Xing JH, Siepmann JI (2000) J Phys Chem B 104:2391
116. Stuart SJ, Berne BJ (1996) J Phys Chem 100:11934
117. Stuart SJ, Berne BJ (1999) J Phys Chem A 103:10300
118. Rick SW, Berne BJ (1996) J Am Chem Soc 118:672
119. Toufar H, Baekelandt BG, Janssens GOA et al (1995) J Phys Chem 99:13876
120. Parr RG, Pearson RG (1983) J Am Chem Soc 105:7512
121. Kitaura K, Morokuma K (1976) Int J Quantum Chem 10:325
122. Weinhold F (1997) J Mol Struct Theochem 398–399:181
123. van der Vaart A, Merz KM (1999) J Am Chem Soc 121:9182
124. Korchowiec J, Uchimaru T (2000) J Chem Phys 112:1623
125. Jeziorski B, Moszynski R, Szalewicz K (1994) Chem Rev 94:1887
126. Chelli R, Procacci P, Righini R et al (1999) J Chem Phys 111:8569
127. Yang ZZ, Wang CS (1997) J Phys Chem A 101:6315
128. Wang CS, Li SM, Yang ZZ (1998) J Mol Struct Theochem 430:191
129. Wang CS, Yang ZZ (1999) J Chem Phys 110:6189
130. Cong Y, Yang ZZ (2000) Chem Phys Lett 316:324
131. Yang ZZ, Wang CS (2003) J Theor Comput Chem 2:273
132. Yang ZZ, Wu Y, Zhao DX (2004) J Chem Phys 120:2541
133. Wu Y, Yang ZZ (2004) J Phys Chem A 108:7563
134. Parr RG, Yang W (1989) Density-Functional Theory of Atoms and Molecules. Oxford University Press, Oxford
135. Field MJ (1997) Mol Phys 91:835
136. Gao JL (1997) J Phys Chem B 101:657
137. Gao JL (1998) J Chem Phys 109:2346
138. van Belle D, Couplet I, Prevost M et al (1987) J Mol Biol 198:721
139. Svishchev IM, Kusalik PG, Wang J et al (1996) J Chem Phys 105:4742
140. Bernardo DN, Ding YB, Kroghjespersen K et al (1994) J Phys Chem 98:4180
141. Medeiros M, Costas ME (1997) J Chem Phys 107:2012
142. Campbell T, Kalia RK, Nakano A et al (1999) Phys Rev Lett 82:4866
143. Car R, Parrinello M (1985) Phys Rev Lett 55:2471
144. van Belle D, Wodak SJ (1995) Comput Phys Comm 91:253
145. Tuckerman ME, Martyna GJ (2000) J Phys Chem B 104:159
146. Tuckerman ME, Martyna GJ (2001) J Phys Chem B 105:7598
147. van Belle D, Froeyen M, Lippens G et al (1992) Mol Phys 77:239
148. Sprik M, Klein ML (1988) J Chem Phys 89:7556
149. Stillinger FH, David CW (1978) J Chem Phys 69:1473
150. Lybrand TP, Kollman PA (1985) J Chem Phys 83:2923
151. Barnes P, Finney JL, Nicholas JD et al (1979) Nature 282:459
152. Rullmann JAC, van Duijnen PT (1988) Mol Phys 63:451
153. Ahlström P, Wallqvist A, Engström S et al (1989) Mol Phys 68:563
154. Cieplak P, Kollman P, Lybrand T (1990) J Chem Phys 92:6755
155. Niesar U, Corongiu G, Clementi E et al (1990) J Phys Chem 94:7949
156. Kuwajima S, Warshel A (1990) J Phys Chem 94:460
157. Caldwell J, Dang LX, Kollman PA (1990) J Am Chem Soc 112:9144
158. Dang LX (1992) J Chem Phys 97:2659
159. Kozack RE, Jordan PC (1992) J Chem Phys 96:3120
160. Wallqvist A, Berne BJ (1993) J Phys Chem 97:13841
161. Brodholt J, Sampoli M, Vallauri R (1995) Mol Phys 85:81
162. Brodholt J, Sampoli M, Vallauri R (1995) Mol Phys 86:149
163. Chialvo AA, Cummings PT (1996) J Chem Phys 105:8274
164. Dang LX, Chang TM (1997) J Chem Phys 106:8149
165. Wallqvist A, Ahlström P, Karlström G (1990) J Phys Chem 94:1649
166. Halley JW, Rustad JR, Rahman A (1993) J Chem Phys 98:4110
167. Corongiu G (1992) Int J Quantum Chem 42:1209
168. Zhu SB, Singh S, Robinson GW (1991) J Chem Phys 95:2791
169. Zhu SB, Yao S, Zhu JB et al (1991) J Phys Chem 95:6211
170. Feyereisen MW, Feller D, Dixon DA (1996) J Phys Chem 100:2993
171. Burnham CJ, Li JC, Xantheas SS et al (1999) J Chem Phys 110:4566
172. Dang LX, Smith DE (1993) J Chem Phys 99:6950
173. Sprik M, Klein ML, Watanabe K (1990) J Phys Chem 94:6483
174. Xantheas SS, Dang LX (1996) J Phys Chem 100:3989
175. Bryce RA, Buesnel R, Hillier IH et al (1997) Chem Phys Lett 279:367
176. Cabarcos OM, Weinheimer CJ, Lisy JM (1999) J Chem Phys 110:8429
177. Baik J, Kim J, Majumdar D et al (1999) J Chem Phys 110:9116
178. Robertson WH, Diken EG, Price EA et al (2003) Science 299:1367
179. Lightstone FC, Schwegler E, Hood RQ et al (2001) Chem Phys Lett 343:549
180. Bako I, Hutter J, Palinkas G (2002) J Chem Phys 117:9838
181. Wallqvist A (1990) Chem Phys Lett 165:437
182. Motakabbir KA, Berkowitz ML (1991) Chem Phys Lett 176:61
183. New MH, Berne BJ (1995) J Am Chem Soc 117:7172
184. Rick SW, Berne BJ (1997) J Phys Chem B 101:10488
185. Soper AK, Phillips MG (1986) Chem Phys 107:47
186. Dore JC (1991) J Mol Struct 250:193
187. Dore JC, Blakey DM (1995) J Mol Liq 65–66:85
188. Soper AK (1997) J Phys: Condens Matter 9:2717
189. Jedlovszky P, Brodholt JP, Bruni F et al (1998) J Chem Phys 108:8528
190. Soper AK (2000) Chem Phys 258:121
191. Nakahara M, Matubayasi N, Wakai C et al (2001) J Mol Liq 90:75
192. Narten AH, Levy HA (1972) In: Franks F (ed) Water a comprehensive treatise. Plenum Press, New York
193. Page DI (1972) In: Franks F (ed) Water a comprehensive treatise. Plenum Press, New York
194. Narten AH, Thiessen WE, Blum L (1982) Science 217:1033
195. Yamanaka K, Yamaguchi T, Wakita H (1994) J Chem Phys 101:9830
196. Hura G, Sorenson JM, Glaeser RM et al (2000) J Chem Phys 113:9140
197. Sorenson JM, Hura G, Glaeser RM et al (2000) J Chem Phys 113:9149
198. Head-Gordon T, Hura G (2002) Chem Rev 102:2651
199. Soper AK, Turner J (1993) Int J Mod Phys B 7:3049
200. Soper AK, Bruni F, Ricci MA (1997) J Chem Phys 106:247
201. Mahoney MW, Jorgensen WL (2000) J Chem Phys 112:8910
202. Corongiu G, Clementi E (1992) J Chem Phys 97:2030
203. Berendsen H, Postma JPM, van Gusteren WF (1981) In: Pullman B et al (eds) Intermolecular forces. Reidel Publishing Company, Dordrecht, The Netherlands
204. Jedlovszky P, Vallauri R (1999) Mol Phys 97:1157
205. Rick SW (2001) J Chem Phys 114:2276

206. Jedlovszky P, Richardi J (1999) J Chem Phys 110:8019
207. Mahoney MW, Jorgensen WL (2001) J Chem Phys 115:10758
208. Saint-Martin H, Hernandez-Cobos J, Ortega-Blake I (2005) J Chem Phys 122:224509
209. Lopez-Lemus J, Chapela GA, Alejandre J (2008) J Chem Phys 128:174703
210. Yezdimer EM, Cummings PT (1999) Mol Phys 97:993
211. Kiyohara K, Gubbins KE, Panagiotopoulos AZ (1998) Mol Phys 94:803
212. Svishchev IM, Hayward TM (1999) J Chem Phys 111:9034
213. Berendsen HJC, Grigera JR, Straatsma TP (1987) J Phys Chem 91:6269
214. Panagiotopoulos AZ (1987) Mol Phys 61:813
215. Hill PG (1990) J Phys Chem Ref Data 19:1233
216. Markovich G, Perera L, Berkowitz ML et al (1996) J Chem Phys 105:2675
217. Klopper W, van Duijneveldt-van de Rijdt J, van Duijneveldt FB (2000) Phys Chem Chem Phys 2:2227
218. Tschumper GS, Leininger ML, Hoffman BC et al (2002) J Chem Phys 116:690
219. Lee HM, Suh SB, Lee JY et al (2000) J Chem Phys 112:9759
220. Xantheas SS, Burnham CJ, Harrison RJ (2002) J Chem Phys 116:1493
221. Kaplan JH (2002) Annu Rev Biochem 71:511
222. Zhang CX, Lippard SJ (2003) Curr Opin Chem Biol 7:481
223. Aleman EA, Lamichhane R, Rueda D (2008) Curr Opin Chem Biol 12:647
224. Al-Hashimi HM, Walter NG (2008) Curr Opin Struct Biol 18:321
225. Chen PR, He C (2008) Curr Opin Chem Biol 12:214
226. Manning GS (1978) Quart Rev Biophys 11:179
227. Scott WG (1999) Curr Opin Chem Biol 3:705
228. Draper DE (2004) Rna-a publication of the Rna society 10:335
229. Bartlett GJ, Borkakoti N, Thornton JM (2003) J Mol Biol 331:829
230. Harris ME, Christian EL (2003) Curr Opin Struct Biol 13:325
231. Sigel RKO, Pyle AM (2007) Chem Rev 107:97
232. Doyle DA, Cabral JM, Pfuetzner RA et al (1998) Science 280:69
233. Dutzler R, Campbell EB, Cadene M et al (2002) Nature 415:287
234. Jiang YX, Lee A, Chen JY et al (2003) Nature 423:33
235. Okada T (1991) J Chem Soc Faraday Trans 87:3027
236. Okada T (1998) Anal Sci 14:469
237. Takeda Y, Kanazawa M, Katsuta S (2000) Anal Sci 16:929
238. Dang LX, Rice JE, Caldwell J et al (1991) J Am Chem Soc 113:2481
239. Roux B (1993) Chem Phys Lett 212:231
240. Roux B, Karplus M (1995) J Comp Chem 16:690
241. Dzidic I, Kebarle P (1970) J Phys Chem 74:1466
242. Marcus Y (1986) J Chem Soc Faraday Trans I 83:233
243. Tissandier MD, Cowen KA, Feng WY et al (1998) J Phys Chem A 102:7787
244. Åqvist J (1990) J Phys Chem 94:8021
245. Cheatham TEIII (2005) In: Spellmeyer DC (ed) Annual reports in computational chemistry. Elsevier, Amsterdam
246. Beglov D, Roux B (1994) J Chem Phys 100:9050
247. Marchand S, Roux B (1998) Protein Struct Funct Genet 33:265
248. Rosseinsky DR (1965) Chem Rev 65:467
249. Kalidas C, Hefter G, Marcus Y (2000) Chem Rev 100:819
250. Grunwald E, Baughman G, Kohnstam G (1960) J Am Chem Soc 82:5801
251. Warren GL, Patel S (2007) J Chem Phys 127:064509
252. Warren GL, Patel S (2008) J Phys Chem C 112:7455
253. Warren GL, Patel S (2008) J Phys Chem B 112:11679
254. Masia M, Probst M, Rey R (2005) J Chem Phys 123:164505
255. Masia M, Probst M, Rey R (2004) J Chem Phys 121:7362
256. Li X, Yang ZZ (2005) J Phys Chem A 109:4102
257. Yang ZZ, Li X (2005) J Phys Chem A 109:3517
258. Piquemal JP, Perera L, Cisneros GA et al (2006) J Chem Phys 125:054511
259. Bagus PS, Illas F (1992) J Chem Phys 96:8962
260. Jungwirth P, Tobias DJ (2006) Chem Rev 106:1259
261. Salvador P, Curtis JE, Tobias DJ et al (2003) Phys Chem Chem Phys 5:3752
262. Archontis G, Leontidis E, Andreou G (2005) J Phys Chem B 109:17957
263. Archontis G, Leontidis E (2006) Chem Phys Lett 420:199
264. Tuma L, Jenicek D, Jungwirth P (2005) Chem Phys Lett 411:70
265. Brown MA, D'Auria R, Kuo IFW et al (2008) Phys Chem Chem Phys 10:4778
266. Wang XW, Watanabe H, Fuji M et al (2008) Chem Phys Lett 458:235
267. Picalek J, Minofar B, Kolafa J et al (2008) Phys Chem Chem Phys 10:5765
268. Hagberg D, Karlstrom G, Roos BO et al (2005) J Am Chem Soc 127:14250
269. No KT, Grant JA, Scheraga HA (1990) J Phys Chem 94:4732
270. No KT, Grant JA, Jhon MS et al (1990) J Phys Chem 94:4740
271. van Belle D, Wodak SJ (1993) J Am Chem Soc 115:647
272. Rick SW (2003) J Phys Chem B 107:9853
273. English NJ, MacElroy JMD (2003) J Comp Chem 24:1569
274. Zhang Q, Yang ZZ (2005) Chem Phys Lett 403:242
275. Borodin O, Smith GD (2006) J Phys Chem B 110:6279
276. Patel SA, Brooks CL (2006) J Chem Phys 124:204706
277. Davis JE, Warren GL, Patel S (2008) J Phys Chem B 112:8298
278. Jalkanen JP, Zerbetto F (2006) J Phys Chem B 110:5595
279. Caldwell JW, Kollman PA (1995) J Phys Chem 99:6208
280. Cieplak P, Caldwell J, Kollman P (2001) J Comp Chem 22:1048
281. Chelli R, Pagliai M, Procacci P et al (2005) J Chem Phys 122
282. Ferenczy GG (1991) J Comp Chem 12:913
283. Winn PJ, Ferenczy GG, Reynolds CA (1997) J Phys Chem A 101:5437
284. Winn PJ, Ferenczy GG, Reynolds CA (1999) J Comp Chem 20:704
285. Kaminski GA, Friesner RA, Zhou RH (2003) J Comp Chem 24:267
286. Yu HB, Geerke DP, Liu HY et al (2006) J Comp Chem 27:1494
287. Valdez-Gonzales M, Saint-Martin H, Hernandez-Cobos J et al (2007) J Chem Phys 127:224507
288. Patel S, Brooks CL (2005) J Chem Phys 123:164502
289. Patel S, Brooks CL (2005) J Chem Phys 122:024508
290. Zhong Y, Warren GL, Patel S (2008) J Comp Chem 29:1142
291. Kaminski GA, Stern HA, Berne BJ et al (2004) J Phys Chem A 108:621
292. Soteras I, Curutchet C, Bidon-Chanal A et al (2007) J Chem Theor Comput 3:1901
293. Mayer A, Astrand PO (2008) J Phys Chem A 112:1277
294. Shirts RB, Stolworthy LD (1994) J Inclusion Phenom Mol Recognit Chem 20:297
295. Rick SW, Stuart SJ, Bader JS et al (1995) J Mol Liq 65–66:31
296. Bader JS, Cortis CM, Berne BJ (1997) J Chem Phys 106:2372
297. Mannfors B, Palmo K, Krimm S (2000) J Mol Struct 556:1
298. Borodin O, Smith GD, Douglas R (2003) J Phys Chem B 107:6824
299. Borodin O, Smith GD (2006) J Phys Chem B 110:6293
300. Borodin O, Smith GD (2006) J Phys Chem B 110:4971
301. Borodin O, Smith GD (2006) Macromolecules 39:1620
302. Borodin O, Smith GD, Fan P (2006) J Phys Chem B 110:22773
303. Borodin O, Smith GD (2007) Macromolecules 40:1252
304. Borodin O, Smith GD, Sewell TD et al (2008) J Phys Chem B 112:734
305. Ding YB, Bernardo DN, Kroghjespersen K et al (1995) J Phys Chem 99:11575

306. Meng EC, Caldwell JW, Kollman PA (1996) J Phys Chem 100:2367
307. Allen TW, Andersen OS, Roux B (2004) Proc Natl Acad Sci USA 101:117
308. Allen TW, Andersen OS, Roux B (2006) Biophys J 90:3447
309. Morita A, Kato S (1999) J Chem Phys 110:11987
310. Schropp B, Tavan P (2008) J Phys Chem B 112:6233
311. Botek E, Giribet C, de Azua MR et al (2008) J Phys Chem A 112:6992
312. Warshel A, Levitt M (1976) J Mol Biol 103:227
313. Warshel A (1979) J Phys Chem 83:1640
314. Warshel A (1981) Biochemistry 20:3167
315. Friesner RA (2006) Adv Protein Chem 72:79
316. Harder E, Kim BC, Friesner RA et al (2005) J Chem Theor Comput 1:169
317. Kim BC, Young T, Harder E et al (2005) J Phys Chem B 109:16529
318. Liang T, Walsh TR (2006) Phys Chem Chem Phys 8:4410
319. Llinas P, Masella M, Stigbrand T et al (2006) Protein Sci 15:1691
320. Wang ZX, Zhang W, Wu C et al (2006) J Comp Chem 27:781
321. Yang ZZ, Zhang Q (2006) J Comp Chem 27:1
322. Guan QM, Yang ZZ (2007) J Theor Comput Chem 6:731
323. Jiang N, Ma J (2008) J Phys Chem A 112:9854
324. Cui BQ, Guan QM, Gong LD et al (2008) Chem J Chin Univ-Chinese 29:585
325. Vorobyov I, Li LB, Allen TW (2008) J Phys Chem B 112:9588
326. Masella M, Borgis D, Cuniasse P (2008) J Comp Chem 29:1707
327. Jiao D, Golubkov PA, Darden TA et al (2008) Proc Natl Acad Sci USA 105:6290
328. Schultheis V, Reichold R, Schropp B et al (2008) J Phys Chem B 112:12217
329. Baucom J, Transue T, Fuentes-Cabrera M et al (2004) J Chem Phys 121:6998
330. Babin V, Baucom J, Darden TA et al (2006) Int J Quantum Chem 106:3260
331. Babin V, Baucom J, Darden TA et al (2006) J Phys Chem B 110:11571
332. Cozmuta I, Mehrez H (2007) J Comput Theor Nanosci 4:349
333. Šponer J, Špačková N (2007) Methods 43:278
334. Stefl R, Cheatham TE, Špačková N et al (2003) Biophys J 85:1787